

---

---

PHASE  
TRANSITIONS

---

---

## Metal–Insulator Phase Transition in Iron-Doped Vanadium Dioxide Thin Films

V. N. Andreev<sup>a,\*</sup> and V. A. Klimov<sup>a</sup>

<sup>a</sup>*Ioffe Institute, Russian Academy of Sciences, St. Petersburg, 194021 Russia*

\**e-mail: vn.andreev.solid@mail.ioffe.ru*

Received May 22, 2018

**Abstract**—The electrical conductivity of polycrystalline  $V_{(1-x)}Fe_xO_2$  films has been investigated in a wide temperature range, which covers both the metal and insulator phase regions. It is shown that with an increase in the iron concentration the metal–insulator phase transition shifts toward lower temperatures, while the temperature range of the transition in doped samples additionally broadens as compared with pure  $VO_2$ . To explain the temperature dependence of the electrical conductivity of the  $V_{(1-x)}Fe_xO_2$  insulator phase, a hopping conductivity model has been used, which takes into account the effect of thermal vibrations of atoms on the resonance integral. The values of parameter  $\epsilon$  have been calculated as a function of the degree of  $VO_2$  doping.

DOI: 10.1134/S1063783418120028

### 1. INTRODUCTION

The stoichiometric vanadium dioxide ( $VO_2$ ) single crystals undergo a metal–insulator phase transition (MIT) at a temperature of  $T_c \approx 340$  K. This results in the drastic change in most physical properties of this compound [1, 2]. At temperatures above 340 K,  $VO_2$  is a metal (tetragonal phase  $R$ ) and its electrical conductivity  $\sigma$  is  $\sim 10^4 \Omega^{-1} \text{cm}^{-1}$  and decreases with increasing temperature, which is typical of metals. Upon cooling below  $T_c$  and during the transition to the monoclinic  $M_1$  phase, the electrical conductivity of vanadium dioxide abruptly drops by five orders of magnitude and, with decreasing temperature, continues decreasing. In thin polycrystalline films, which are preferable for creating specific devices, the MIT properties are generally retained, but the parameters of the transition somewhat change. In particular, the electrical conductivity jump decreases by up to three orders of magnitude and the transition is spread in the steep middle MIT part by several degrees, while at the edges of the transition this spread is over 10 K. A powerful factor affecting the MIT in  $VO_2$  is doping. Dopants work as substitutes and can be divided into two groups, group Nb and group Cr, according to the character of their action on the phase transition: group Nb and group Cr. Group Nb includes Mo, W, and Re, the action of which is mainly reduced to decreasing the phase transition temperature. No new low-temperature phases, except for the  $M_1$  phase, form. A decrease in  $T_c$  upon doping with these impurities is attributed to an increase in the lattice parameters and formation of  $V^{3+}$  ions [3–5]. Group Cr includes Al, Fe, and Ga. These

additives convert  $V^{4+}$  in the lattice to  $V^{5+}$  and stabilize two new low-temperature phases,  $M_2$  and  $T$ , the phase diagram of which was obtained in [6]. The monoclinic  $M_1$  phase can be presented as a result of two distortions: pairing of V atoms along the  $(001)_R$  axis and zigzag distortion along the oxygen octahedron axes. In the monoclinic  $M_2$  phase, a half of V atoms (sublattice A) are paired and arranged along the  $(001)_R$  axis, while the other half (sublattice B) forms zigzag chains along the same direction. The triclinic  $T$  phase is characterized by an increase in the slopes in sublattice A and an increase in the zigzag chain dimerization in sublattice B, which eventually leads to equivalent sublattices A and B in the  $M_1$  phase. We would like to emphasize that impurity cations are considered to be not simply donors or acceptors, but centers of internal crystal structure expansion or contraction, respectively, and the presence of internal or external elastic stresses strongly affects the MIT in vanadium dioxide [7–9].

In recent years, the study of doped vanadium dioxide single crystals and thin films has attracted much attention, since it may explain the nature of the phase transition [10–13]. In addition, the interest in this compound is due to the development of nanotechnologies [7].

Although  $VO_2$  has been intensively investigated for the last few decades, the question about the MIT nature in this compound is still unanswered, the effect of electron–phonon interaction and electron correlations on the characteristics of this oxide remain unclear, and the experimental data on the electrical conductivity of pure and doped vanadium dioxide are

fragmentary and have been obtained in a narrow temperature range. Previously, we investigated the electrical conductivity of pure vanadium dioxide in a wide temperature range and showed that the electric transport in  $\text{VO}_2$  is implemented via hoppings of small-radius polarons, which are affected by thermal lattice vibrations [1]. In this study, we investigate the properties of iron-doped vanadium dioxide within this approach.

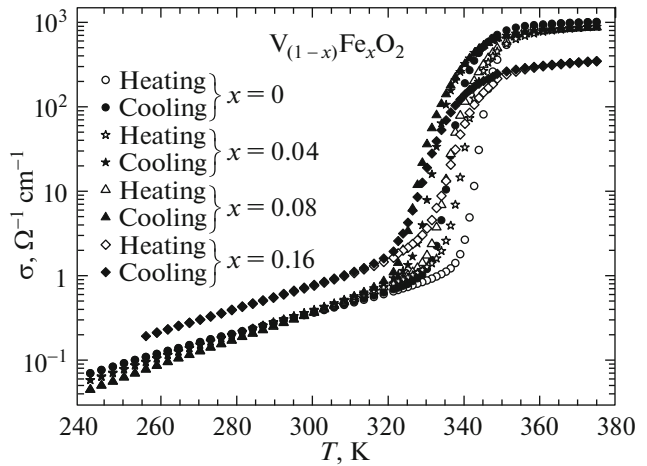
## 2. EXPERIMENTAL

Vanadium dioxide  $\text{V}_{(1-x)}\text{Fe}_x\text{O}_2$  thin films were synthesized by simultaneous laser sputtering of metallic V (99.9%) and metallic Fe (99.8%) targets in the oxygen atmosphere at temperatures of 750–900 K. Since the vanadium and iron melting points are similar, the degree of doping ( $x$ ) was judged by the relative time of evaporation of each target. Sapphire ( $\text{Al}_2\text{O}_3$ ) was used as a substrate material. The film thickness was 50–60 nm.

The temperature phase transition was followed by the variation in the reflectivity of the investigated films at a wavelength of  $\lambda = 1.54 \mu\text{m}$  and in their electrical conductivity measured using a standard four-probe technique. In the latter case, platinum electrodes were deposited onto a substrate before film synthesis by vacuum laser sputtering.

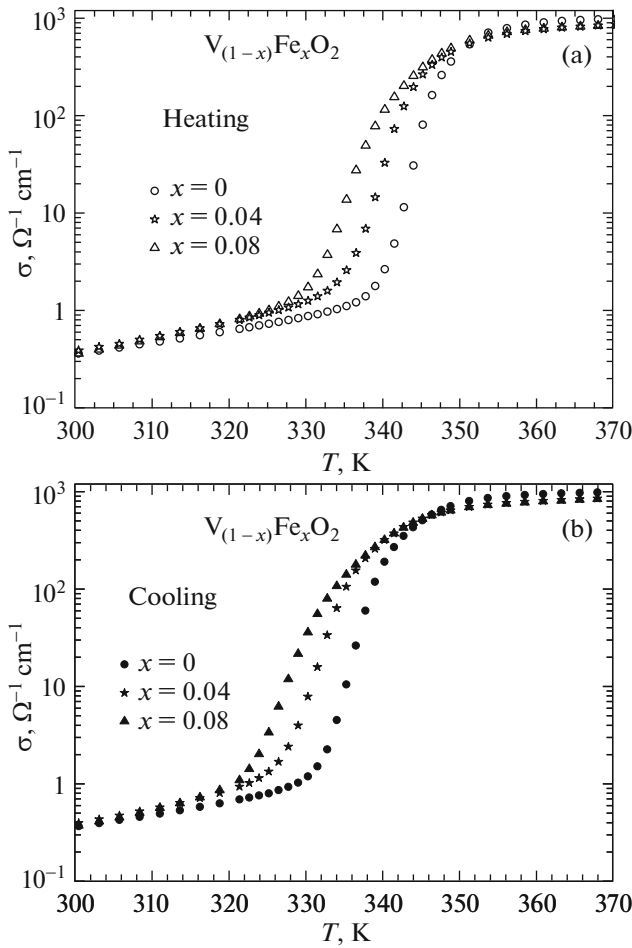
## 3. RESULTS AND DISCUSSION

Figure 1 shows temperature dependences of the electrical conductivity of pure and iron-doped vanadium dioxide. It can be seen that as the iron concentration increases, the MIT temperature shifts toward lower temperatures. At the low impurity concentrations, the MIT parameters, except for  $T_c$ , remain almost invariable. As in pure  $\text{VO}_2$ , the electrical conductivity jump in the doped samples is three orders of magnitude and the hysteresis width remains 8 K. However, with a further increase in the iron concentration, the MIT starts degrading, which manifests itself as a significant decrease in the electrical conductivity jump and transition region broadening, but the MIT temperature no longer shifts toward lower temperatures. This is apparently due to the weakening of the first-order phase transition and its gradual transformation to a second-order transition, because of smearing of the phase boundaries of the  $M_1$ ,  $M_2$ , and  $T$  insulator phases. We do not discuss the MIT degradation at the high impurity concentrations, but investigate in detail the iron concentration regions where the MIT parameters are almost invariable and only the temperature  $T_c$  shifts. Figures 2a and 2b show the  $\sigma(T)$  dependences in the MIT region upon heating and cooling for pure  $\text{VO}_2$  and  $\text{V}_{(1-x)}\text{Fe}_x\text{O}_2$  ( $x = 0.04$  and  $0.08$ ). It is worth noting that, in our case, the impurity concentration is much higher than in [6]. The electri-



**Fig. 1.** Temperature dependences of the electrical conductivity of the  $\text{V}_{(1-x)}\text{Fe}_x\text{O}_2$  films with different iron concentrations.

cal conductivity in the metal phase for the investigated samples is  $\sigma_m \sim 10^3 \Omega^{-1} \text{cm}^{-1}$ , which is similar to the Mott minimum metal conductivity limit [14], but the behavior of  $\sigma(T)$  is atypical of metals. This is apparently due to the Anderson localization caused by inhomogeneities of the grain composition and defects in the grain boundaries (the films are polycrystalline). Note that in single crystals the metal-type conductivity is observed ( $\sigma_m \sim 10^4 \Omega^{-1} \text{cm}^{-1}$ ) [1]. The phase transition in a polycrystalline film differs from that in a single crystal not only by the  $\sigma$  jump, but also by the shape of the temperature dependence of the transition. In a single crystal, this is a vertical line caused by the avalanche-like transition over the entire sample volume. In a polycrystalline film, the avalanche-like transition occurs independently in the bulk of each grain; therefore, the  $\sigma(T)$  line in the MIT region, even in its steepest middle part, is spread by  $\Delta T \sim 8 \text{K}$ . In addition, at the beginning and end of the transition, there are wings extended by  $\Delta T \sim 20 \text{K}$ . The hysteresis width in our films is  $\Delta T \sim 8 \text{K}$  and the MIT temperature range is extended to  $\Delta T \sim 50 \text{K}$  (the distance between the points where the forward and backward hysteresis branches merge). In addition, the MIT region broadening is influenced by the flow effects [15]. Therefore, in the temperature dependences of the film reflectivity, where there are no flow effects, this region is narrower. The comparison of the hysteresis branch shapes upon heating and cooling for pure and doped  $\text{VO}_2$  (Fig. 2) shows that in  $\text{V}_{(1-x)}\text{Fe}_x\text{O}_2$ , the upper third of the hysteresis branches is excessively spread and tilted toward high temperatures, covering a part of the high-temperature hysteresis wing. This is probably due to the MIT splitting caused by a successive transition of the  $R$ – $M_2$  and  $M_2$ – $T$  interfaces. Due to the temperature spread, these transitions merge,



**Fig. 2.** Temperature dependences of the electrical conductivity of the pure and iron-doped  $\text{VO}_2$  films in the phase transition region obtained upon (a) heating and (b) cooling.

but, as compared with pure  $\text{VO}_2$ , where there is the only interface  $R-M_1$ , such a mechanism seems reasonable. It should be noted that when measuring the magnetic susceptibility of  $\text{V}_{(1-x)}\text{Fe}_x\text{O}_2$ , a double transition was also observed [16].

Figure 1 shows the measured electrical conductivities of pure and iron-doped  $\text{VO}_2$  after the transition to the insulator phase upon cooling to a temperature of  $T = 240$  K. It can be seen that the  $\sigma(T)$  dependence is linear in the coordinates  $\log(\sigma)$  on  $T$ . Previously, we investigated the electrical conductivity of vanadium dioxide and demonstrated that its conductivity is described by hoppings of small-radius polarons affected by thermal lattice vibrations [1]. Since the charge transfer mechanism in the insulator phase should not change upon doping of vanadium dioxide, it is reasonable to study the electrical conductivity of  $\text{V}_{(1-x)}\text{Fe}_x\text{O}_2$  in the framework of the Bryksin's model [17], which takes into account thermal displacements of the lattice atoms on the probability of interstitial

hoppings of small polarons. The atomic displacements change the overlap of wave functions of the states on neighboring sites. This overlap determines the resonant integral  $I$ . In the first approximation,  $I$  changes with the hopping distance  $R$  as  $\exp(-\alpha R)$ , where  $\alpha^{-1}$  is the effective localization radius. The hopping mobility of a carrier, which determines the electrical conductivity of vanadium dioxide, is, in turn, proportional to  $I^2$ . At small  $\alpha^{-1}$  values comparable with the lattice vibration amplitude  $\rho$ , we may assume  $I^2$  to depend linearly on  $\rho$ . Therefore, for the dependence of  $I^2$  on  $\rho$ ,  $I^2$  can be replaced by  $\langle I^2 \rangle$ , where the angular brackets denote phonon averaging via the Debye–Waller factor renormalization.

$$\langle I^2 \rangle = I^2 \exp(2\alpha^2 \langle \rho^2 \rangle), \quad (1)$$

where  $\langle \rho^2 \rangle$  is the root-mean-square thermal displacement of atoms on the lattice sites. The calculation of the hopping conductivity using the small-radius polaron model with regard to the effect of thermal lattice vibrations on the resonance integral yields the following temperature dependence of the electrical conductivity:

$$\sigma = en \frac{ea^2}{2h} \frac{\pi^{1/2} I^2}{E_a^{1/2} (k_B T)^{3/2}} \exp\{-E_a/k_B T + k_B T/\varepsilon\}, \quad (2)$$

where  $a$  is the lattice constant,  $E_a$  is the energy required for electron hopping,  $n$  is the carrier density,  $e$  is the elementary charge,  $h$  is Planck's constant, and  $\varepsilon$  is the quantity with the energy dimension, which takes into account the effect of thermal lattice vibrations on the resonance integral. In the high-temperature region, where we have  $2k_B T > \hbar\omega_q$  ( $\hbar = h/2\pi$  and  $\omega_q$  is the optical phonon frequency),  $\varepsilon$  is related to the root-mean-square thermal displacement  $\langle \rho^2 \rangle$  as

$$\varepsilon = k_B T / 2\alpha^2 \langle \rho^2 \rangle. \quad (3)$$

Analysis of Eq. (2) shows that at low temperatures the second term under the exponent becomes negligible as compared with the first term, while at high temperatures the second term dominates. Therefore, in the low-temperature limit, Eq. (2) can be written in the form

$$\ln(\sigma T^{3/2}) = A - E_a/k_B T, \quad (4)$$

where  $A$  and  $E_a$  are temperature-independent.

On the contrary, in the high-temperature limit, Eq. (2) can be presented in the form

$$\ln(\sigma T^{3/2}) = A + k_B T/\varepsilon, \quad (5)$$

where  $A$  and  $\varepsilon$  are temperature-independent.

As we showed in [1], at temperatures above  $T \sim 240$  K,  $\sigma(T)$  for  $\text{VO}_2$  can be described by dependence (5). This dependence for  $\text{VO}_2$  and  $\text{V}_{(1-x)}\text{Fe}_x\text{O}_2$  ( $x = 0.04$  and  $0.08$ ) is shown in Fig. 3. It can be seen that with an increase in the iron concentration, the slope of

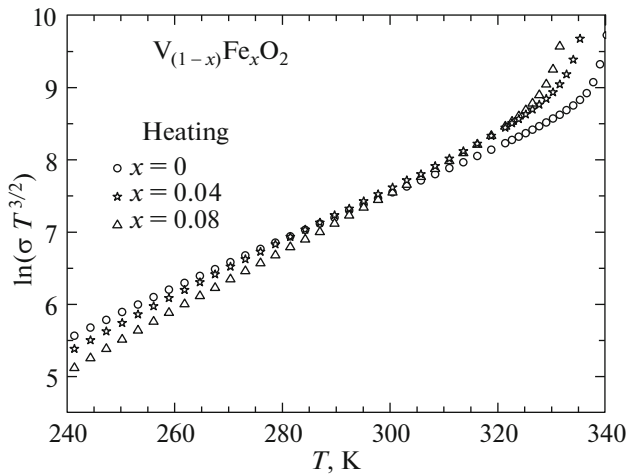


**Fig. 3.** Dependence  $\ln(\sigma T^{3/2}) = A + k_B T/\varepsilon$  for the  $V_{(1-x)}Fe_xO_2$  films with different iron concentrations.

the straight line equal to  $\varepsilon^{-1}$ , increases. The  $\varepsilon$  values for  $VO_2$  and  $V_{(1-x)}Fe_xO_2$  ( $x = 0.04$  and  $0.08$ ) were found to be  $2.72 \times 10^{-3}$  eV,  $2.35 \times 10^{-3}$  eV, and  $2.15 \times 10^{-3}$  eV, respectively. The  $\varepsilon^{-1}$  value is proportional to the time of tunneling of a small polaron through a barrier between neighboring sites. In other words, the polaron mobility increases with a decrease in the  $\varepsilon^{-1}$  value. According to our data, as the iron concentration in vanadium dioxide increases, the  $\varepsilon^{-1}$  value also increases, which can be interpreted as an increase in the carrier localization on a site due to the crystal lattice expansion, which leads to a decrease in the MIT temperature.

#### 4. CONCLUSIONS

It was shown that iron doping of vanadium dioxide significantly changes the temperature dependence of the electrical conductivity of  $V_{(1-x)}Fe_xO_2$  as compared with pure  $VO_2$ . It was shown that the additional  $\sigma(T)$  spread in the MIT region upon approaching the metal phase in the doped  $VO_2$  samples can be caused by the formation of additional interfaces,  $R-M_2$  and  $M_2-T$ . The electrical conductivity of the  $V_{(1-x)}Fe_xO_2$  insulator phase is described well by the small polaron model, which takes into account the effect of thermal vibrations of the lattice atoms on the resonance integral. The characteristic model parameter  $\varepsilon$  for pure and doped  $VO_2$  was determined. It was demonstrated that the energy  $\varepsilon$ , which takes into account the effect of thermal vibrations of the lattice on the probability of tunneling of a small polaron through a barrier between

neighboring sites, decreases with increasing dopant concentration. This is, probably, due to an increase in the lattice parameters.

#### ACKNOWLEDGMENTS

This study was supported in part by the Program of the Physical Sciences Division, Russian Academy of Sciences.

#### REFERENCES

1. V. N. Andreev and V. A. Klimov, *Phys. Solid State* **49**, 2251 (2007).
2. A. Zilbersztein and N. F. Mott, *Phys. Rev. B* **11**, 4383 (1975).
3. V. N. Andreev and V. A. Klimov, *Phys. Solid State* **58**, 606 (2016).
4. G. Villeneuve, A. Bordet, A. Casalot, J. P. Pouget, H. Launois, and P. Lederer, *J. Phys. Chem. Solids* **33**, 1953 (1972).
5. M. Ritschel, N. Mattern, W. Bruckner, H. Oppermann, G. Strover, W. Moldenhauer, J. Henre, and E. Wolf, *Krist. Technol.* **12**, 1221 (1977).
6. M. Marezio, D. B. McWhan, J. P. Remeika, and P. D. Dernier, *Phys. Rev. B* **7**, 2541 (1972).
7. J. H. Park, J. M. Coy, T. S. Kasirga, C. Huang, Z. Fei, S. Hunter, and D. H. Gobden, *Nature (London, U.K.)* **500**, 431 (2013).
8. J. Wu, Q. Gu, B. S. Guiton, N. P. de Leon, L. Ouyang, and H. Park, *Nano Lett.* **6**, 2313 (2006).
9. A. Tselev, I. A. Luk'yanchuk, I. N. Ivanov, J. D. Budai, J. Z. Tischler, E. Strelkov, K. Jones, A. Kolmakov, and S. V. Kalinin, *Nano Lett.* **10**, 4409 (2010).
10. E. Strelkov, A. Tselev, I. Ivanov, J. D. Budai, J. Zhang, J. Z. Tischler, I. Kravchenko, S. V. Kalinin, and A. Kolmakov, *Nano Lett.* **12**, 6198 (2012).
11. T. J. Hanlon, J. A. Coath, and M. A. Richardson, *Thin Solid Films* **436**, 269 (2003).
12. C. Marini, E. Arcangeletti, D. di Castro, L. Baldassare, A. Perucchi, S. Lupi, L. Malavasi, L. Boeri, E. Pomjakushina, K. Conder, and P. Postorino, *Phys. Rev. B* **77**, 235111 (2008).
13. V. N. Andreev, V. A. Klimov, M. E. Kompan, and B. A. Melekh, *Phys. Solid State* **56**, 1857 (2014).
14. N. F. Mott, *Metal–Insulator Transitions* (Taylor and Francis, London, 1974).
15. V. N. Andreev, T. V. Smirnova, and F. A. Chudnovskii, *Phys. Status Solidi B* **77**, K97 (1977).
16. E. Pollert, G. Villeneuve, F. Menil, and P. Hagenmuller, *Mater. Res. Bull.* **11**, 159 (1976).
17. V. V. Bryksin, *Sov. Phys. JETP* **73**, 861 (1991).

*Translated by E. Bondareva*